MOLECULAR AND CELLULAR BIOLOGY, Apr. 1999, p. 3145–3155 Vol. 19, No. 4
0270-7306/99/$04.00+0

SAG, a Novel Zinc RING Finger Protein That Protects Cells from Apoptosis Induced by Redox Agents

HANGJUN DUAN,[1] YULI WANG,[1] MICHEAL AVIRAM,[2]† MANJU SWAROOP,[1] JOSEPH A. LOO,[3] JUNHUI BIAN,[1]‡ YE TIAN,[1] TOM MUELLER,[1] CHARLES L. BISGAIER,[2]§ AND YI SUN[1]*

Departments of Molecular Biology,[1] Cardiac and Vascular Diseases,[2] and Chemistry,[3] Parke-Davis Pharmaceutical Research, Division of Warner-Lambert Company, Ann Arbor, Michigan 48105

Received 18 November 1998/Returned for modification 22 December 1998/Accepted 11 January 1999

***SAG* (sensitive to apoptosis gene) was cloned as an inducible gene by 1,10-phenanthroline (OP), a redox-sensitive compound and an apoptosis inducer. *SAG* encodes a novel zinc RING finger protein that consists of 113 amino acids with a calculated molecular mass of 12.6 kDa. SAG is highly conserved during evolution, with identities of 70% between human and *Caenorhabditis elegans* sequences and 55% between human and yeast sequences. In human tissues, *SAG* is ubiquitously expressed at high levels in skeletal muscles, heart, and testis. SAG is localized in both the cytoplasm and the nucleus of cells, and its gene was mapped to chromosome 3q22-24. Bacterially expressed and purified human SAG binds to zinc and copper metal ions and prevents lipid peroxidation induced by copper or a free radical generator. When overexpressed in several human cell lines, SAG protects cells from apoptosis induced by redox agents (the metal chelator OP and zinc or copper metal ions). Mechanistically, SAG appears to inhibit and/or delay metal ion-induced cytochrome *c* release and caspase activation. Thus, SAG is a cellular protective molecule that appears to act as an antioxidant to inhibit apoptosis induced by metal ions and reactive oxygen species.**

Reactive oxygen species (ROS) are a group of very reactive, short-lived chemicals produced during normal respiratory processes or after oxidative insults. ROS include superoxide anion, hydrogen peroxide, hydroxyl radical, and organic peroxides, among others (56). ROS, at low concentrations, have been implicated in the regulation of several physiological processes such as proliferation (55), differentiation (3), apoptosis (25), and senescence (14). At high concentrations, ROS are highly toxic to cells, by inducing DNA damage, lipid peroxidation, and protein degradation (56). Several lines of evidence suggest that ROS may mediate apoptosis: (i) the production of ROS or depletion of antioxidants promotes apoptosis (43, 64); (ii) antioxidants inhibit apoptosis (43, 64), and (iii) generation of ROS mediates p53-induced apoptosis (48). ROS appear to function mainly at the initiation/activation step of apoptosis since most apoptosis inducers produce ROS. Examples include irradiation, UV, chemicals, ceramides, and growth factor withdrawal, among many others (28, 66). How do ROS, as the highly reactive but nonspecific molecules, mediate well-coordinated apoptosis? It is unlikely that ROS themselves are direct signaling molecules that activate some crucial components of apoptosis machinery due to their lack of biological specificity. More likely, ROS act indirectly by modifying cellular redox-sensitive molecules, such as p53 and NF-κB, that are directly involved in apoptosis (6, 42, 58, 61).

Metal chelators and metal ions are redox-sensitive agents that could mediate ROS generation through the Fenton reaction. 1,10-Phenanthroline (OP), a typical metal chelator (4), has been previously shown to either induce or suppress apoptosis in a cell line-dependent manner (1, 2, 7, 41). OP induces apoptosis by increasing expression of cell surface APO/Fas ligand (41), by chelating zinc (2, 26), or by chelating copper and promoting its redox activity to induce internucleosomal DNA fragmentation (11, 67). Copper ion (Cu^{2+}) is a highly reactive ion that has been used in concert with OP, chemicals, or carcinogens to induce apoptosis in a number of cellular models (11, 24, 51, 53, 67, 70). Cu^{2+} is readily reduced to Cu^{+}, and the latter reacts with H_2O_2 through the Fenton reaction to form the highly toxic hydroxyl radical that causes cell death (71). The zinc ion, however, is a rather stable trace element. It has been found that zinc can either induce or suppress apoptosis in a concentration-dependent manner (19, 49). High concentrations of extracellular zinc (500 to 1,000 μM) suppress apoptosis, probably by either inhibiting a Ca^{2+}/Mg^{2+}-dependent endonuclease, which is responsible for DNA fragmentation (73), or by inhibiting caspase 3 (47). At lower concentrations (80 to 200 μM), zinc appears to induce apoptosis (19, 49), most likely by enhancing the generation of hydroxyl free radicals (46). Furthermore, zinc induces neuronal death both in cultured cells (12, 31, 39) and in animals (32).

To counteract the damaging effects of ROS, aerobic cells are endowed with extensive antioxidant defense systems. These defense systems consist mainly of antioxidant enzymes (e.g., superoxide dismutase, catalase, glutathione peroxidase, and glutathione reductase), antioxidant proteins (e.g., thioredoxin and metallothionein [MT]), and small molecular antioxidants (e.g., glutathione, *N*-acetyl-L-cysteine, and vitamin C). Almost all antioxidant molecules have been shown to protect cells against apoptosis induced by redox-sensitive reagents (5, 29, 33, 40).

In an attempt to understand signaling pathways leading to apoptosis induced by OP, a metal-chelating and redox-sensitive reagent (58), we used the differential display (DD) technique for identification of OP-responsive genes and reported the cloning of an OP-inducible gene that encodes glutathione synthetase (GSS) (57). Here we report the cloning and char-

* Corresponding author. Mailing address: Department of Molecular Biology, Parke-Davis Pharmaceutical Research, Division of Warner-Lambert Company, 2800 Plymouth Road, Ann Arbor, MI 48105. Phone: (734) 622-1959. Fax: (734) 622-7158. E-mail: yi.sun@wl.com.

† Present address: Lipid Research Laboratory, Rambam Medical Center, Bat-Galim, Haifa 31096, Israel.

‡ Present address: Abilene Christian University, Abilene, TX 79699.

§ Present address: Esperion Therapeutic, Inc., Ann Arbor, MI 48108.

acterization of second OP-inducible gene which encodes SAG (sensitive to apoptosis gene), an evolutionarily conserved novel zinc RING finger protein with features of metal ion binding and free radical scavenging. When overexpressed in several human cell lines, SAG protects cells against apoptosis induced by OP, zinc, and copper. Thus, SAG appears to function as an antioxidant molecule to inhibit metal ion- or ROS-induced apoptosis.

MATERIALS AND METHODS

Cell maintenance and drug treatment. Human neuroblastoma line SY5Y and human kidney line 293 were cultured in Dulbecco's modified Eagle medium containing 10% fetal calf serum (FCS; Sigma). Human colon carcinoma line DLD-1 was grown in Eagle minimal essential medium (MEM) containing 10% FCS. Two mouse tumor lines, L-RT101 and H-Tx, were used. L-RT101, a tumor promoter-transformed JB6 epidermal line (62), was cultured in Eagle MEM containing, FCS; H-Tx, a spontaneously transformed liver line (59a), was grown in Dulbecco's modified Eagle medium supplemented with 10% FCS and 1 mM sodium pyruvate. For drug treatment, subconfluent cells were exposed to dimethyl sulfoxide vehicle control, OP or metal ions, zinc sulfate, or copper sulfate (Sigma) for various periods of time up to 24 h.

DD. Analysis was performed by using an RNAimage kit B (GeneHunter) as instructed by the manufacturer, with slight modification (59). Briefly, total RNA was isolated by using RNAzol solution (Tel-Test) and subjected to reverse transcription followed by PCR. PCR fragments were resolved in sequencing gels. The fragments reproducibly showing differential expression were PCR amplified and used as probes for Northern analysis. Northern analysis-confirmed fragments were then subcloned into TA cloning vector (Invitrogen) and sequenced by using DNA Sequenase version 2.0 (Amersham). The GenBank search was performed with the Genetics Computer Group program.

cDNA library screening and 5′ rapid amplification of cDNA ends. The mouse lung cDNA library (Stratagene) was screened with a DD fragment to clone full-length mouse *SAG* (*mSAG*). The longest clone isolated was a 1.0-kb fragment consisting of partial open reading frame and the entire 3′-end untranslated region. A mouse brain Marathon-Ready cDNA (Clontech) was used to clone the 5′-end upstream sequence, which yielded a 100-bp fragment consisting of the 5′-end untranslated sequence and some of the coding sequence. To clone human *SAG* (*hSAG*), the 1.0-kb *mSAG* fragment was used as a probe to screen a human HeLa cDNA library (Stratagene). A 0.75-kb fragment flanking the entire open reading frame and some 3′-end untranslated region was obtained.

Cellular localization by immunofluorescence. Cells were plated on coverslips in 24-well culture dishes and transfected by the calcium phosphate method with the following constructs: pcDNA3.1 (vector control with a Myc-His tag; Invitrogen); pcDNA3.1-SAG (*SAG* cDNA cloned upstream and in frame with Myc-His tag); or pcDNA3.1-LacZ. Two days posttransfection, cells were washed with cold phosphate-buffered saline (PBS) and fixed with 3% formaldehyde in PBS for 10 min followed by 5 min in methanol-acetone (1:1). The fixed cells were washed with PBS four times and incubated with Myc tag antibody (1:200 dilution; Invitrogen) in PBS containing 1% bovine serum albumin, 0.1% saponin, and 2 μg of 4′,6-diamidino-2-phenylindole (DAPI) per ml for 1 h in the dark with shaking. Cells were then washed with 0.1% saponin in PBS and incubated with fluorescein isothiocyanate (FITC)-conjugated goat anti-mouse antibody (1:100 dilution; Jackson Laboratory) for 1 h in the same condition as the first antibody. After incubation, cells were washed first with 0.1% saponin in PBS and then with PBS. The coverslips were mounted to glass slides with nonfade mounting medium and analyzed in a Leica Dialux 20 microscope.

Fluorescence in situ hybridization (FISH) chromosome mapping. (i) Slide preparation. Lymphocytes isolated from human blood were cultured in MEM supplemented with 10% FCS and phytohemagglutinin (PHA) at 37°C for 68 to 72 h. The lymphocyte cultures were treated with bromodeoxyuridine (0.18 mg/ml; Sigma) to synchronize the cell population. The synchronized cells were washed with serum-free medium and recultured at 37°C for 6 h in α-MEM with thymidine (2.5 μg/ml; Sigma). Cell were harvested, and slides were made by using standard procedures including hypotonic treatment, fixation, and air drying.

(ii) In situ hybridization and FISH detection. A 750-bp *hSAG* cDNA probe was biotinylated with dATP, using the Bethesda Research Laboratories BioNick labeling kit (15°C, 1 h) (22). FISH detection was performed as described previously (22, 23). Briefly, slides were baked at 55°C for 1 h. After RNase treatment, the slides were denatured in 70% formamide in 2× SSC (1× SSC is 0.15 M NaCl plus 0.015 M sodium citrate) for 2 min at 70°C followed by dehydration with ethanol. Probes were denatured at 75°C for 5 min in a hybridization mix consisting of 50% formamide and 10% dextran sulfate. Probes were loaded on the denatured chromosomal slides. After overnight hybridization, slides were washed and signals were detected. FISH signals and the DAPI banding pattern were recorded separately by taking photographs, and FISH mapping data were correlated with chromosomal bands by superimposing FISH signals with DAPI-banded chromosomes.

ESI-MS. Electrospray ionization mass spectrometry (ESI-MS) was performed with a double-focusing hybrid mass spectrometer (MAT 900Q; Finnigan, Bremen, Germany) with a mass-to-charge range of 10,000 at 5-kV full acceleration potential. A position-and-time-resolved-ion-counting (PATRIC) scanning array detector was used. An ESI interface based on a heated metal capillary inlet and a low-flow micro ESI source (analyte flow rate of 150 nl min^{-1}) were used (50). The metal capillary temperature was maintained at around 150 to 200°C for metal-protein complex studies. Recombinant protein in a 7 M urea-denaturing solution was refolded by dialysis in 50 μM $ZnSO_4$ for 3 days with three changes of buffer. Prior to ESI-MS measurement, the SAG solution was washed with a solution of 10 mM ammonium bicarbonate (pH 7) and 1 mM dithiothreitol (DTT), and excess zinc was removed by centrifugal ultrafiltration by passage through a 10-kDa-molecular-mass cutoff centrifugal filtration cartridge (Microcon-10 microconcentrator; Amicon, Beverly, Mass.). For ESI-MS analysis, a small portion of the filtered SAG protein solution was diluted into either a denaturing solvent (80:15:5 [vol/vol/vol] acetonitrile-water-acetic acid [pH 2.5]) or a nondenaturing solution (10 mM ammonium bicarbonate, 1 mM DTT [pH 7]).

Assay for lipoprotein oxidation. Lipoproteins (100 μg of protein/ml; Intraocel) were incubated with 10 μM $CuSO_4$ or with 5 mM 2,2-azo-bis-2-amidinopropane hydrochloride (AAPH) for 4 h at 37°C in the presence of various concentrations of purified SAG protein. AAPH is a water-soluble azo compound that thermally decomposes and generates water-soluble peroxyl radicals at a constant rate (21). Oxidation was terminated by the addition of 10 μM butylated hydroxytoluene and refrigeration at 4°C. The extent of lipoprotein oxidation was measured by the thiobarbituric acid-reactive substances (TBARS) assay, using malondialdehyde for the standard curve, as described previously (10).

Antibody generation. Two polyclonal antibodies against hSAG protein were generated, using standard methods, by Zymed Laboratories, Inc. (San Francisco, Calif.). Briefly, the peptide antibody was generated as following. A 16-amino-acid peptide (SAG-Pepl; QNNRCPLCQQDWWQR) located in the C terminus of SAG protein (codons 95 to 110) was synthesized and purified via standard techniques. The purified peptide was conjugated to keyhole limpet hemocyanin via cysteine residues. The conjugated peptide (0.5 mg) was emulsified with an equal volume of complete Freund's adjuvant and subcutaneously injected into rabbits, followed by four boosts with 0.5 mg each in incomplete Freund's adjuvant at 3-week intervals. Rabbits were bled 10 days after the final boost, and antiserum was collected. The same protocol was used for protein antibody production using bacterially expressed and purified hSAG protein as the antigen.

Preparation of subcellular fractions. Subcellular fractions of the D1-6 and D12-1 cells or 293 transfectants were prepared as described previously (74). Briefly, the cells were harvested after exposure to $ZnSO_4$ or $CuSO_4$ for various periods of time and washed twice with ice-cold PBS. The cell pellet was resuspended in 5 volumes of cold buffer A (20 mM HEPES-KOH [pH 7.5], 10 mM KCl, 1.5 mM $MgCl_2$, 1 mM sodium EDTA, 1 mM sodium EGTA, 1 mM DTT, and 0.1 mM phenylmethylsulfonyl fluoride) containing 250 mM sucrose and freshly added protease inhibitor cocktail (Boehringer Mannheim). After homogenization for 10 strokes with a Dounce homogenizer, the nuclei were discarded by centrifugation at 1,000 × *g* for 10 min at 4°C. The supernatant was further centrifuged at 10,000 × *g* for 15 min at 4°C, and the resulting supernatants were used for protein and immunoblot assays.

Immunoblot assay. The cytosolic proteins (50 μg) prepared as described above were resolved on a sodium dodecyl sulfate-polyacrylamide gel and transferred to a polyvinylidene difluoride membrane. Immunoblots were probed with a monoclonal antibody against caspase 3 (Transduction Laboratories), a monoclonal antibody against human cytochrome *c* (PharMingen), or a rabbit polyclonal antibody against caspase 7 (15). For SAG detection, either rabbit anti-SAG antibody (1:1,000 dilution) or Flag antibody (Sigma) was used. Proteins were detected by horseradish peroxidase-conjugated secondary antibody coupled with enhanced chemiluminescence Western blotting detection reagents (Amersham).

Northern analysis and immunoprecipitation. The assays were performed as detailed previously (60, 62). Briefly, total RNA was isolated and subjected to Northern analysis using *mSAG* and *hSAG* cDNA as probes. For immunoprecipitation, subconfluent *SAG* transfectants and the vector control cells were subjected to methionine starvation for 1 h and metabolically labeled with Trans[^{35}S]-label (0.2 mCi/ml) for 3 h. Cells were then lysed on ice for 30 min in lysis buffer (60) and spun at 12,000 × *g*. The equal counts of trichloroacetic acid-precipitable radioactivity in the supernatant (3×10^7 cpm) were immunoprecipitated with rabbit anti-human SAG antibody. The immunoprecipitates were then collected, washed, and analyzed by separation on a sodium dodecyl sulfate–10 to 20% polyacrylamide gel followed by autoradiography. Densitometric quantitation was performed on a densitometer (Molecular Dynamics).

Construction of *SAG* expression vectors and establishment of stable expressing clones. Reverse transcription-PCR (60) was performed to clone the *hSAG* coding region into the following expression vectors: pcDNA 3C (containing a Myc tag; Invitrogen), for immunolocalization study; and pcDNA3 (Invitrogen), for stable transfection in DLD-1 cells. To generate a Flag-tagged *SAG* expression construct, *hSAG* cDNA was PCR amplified by using primers Flag-SAG (5′-CGGGGTACCGCCATGGACTACAAGGACGACGATGACAAGGCCGACGTGGAAGAC-3′) and SAG-XhoI (5′-CCGCTCGAGTCATTTGCCGATTCTTTGGACCAC-3′). The PCR fragment was subcloned into pcDNA3. All PCR-generated clones were verified by DNA sequencing for appropriate orientation

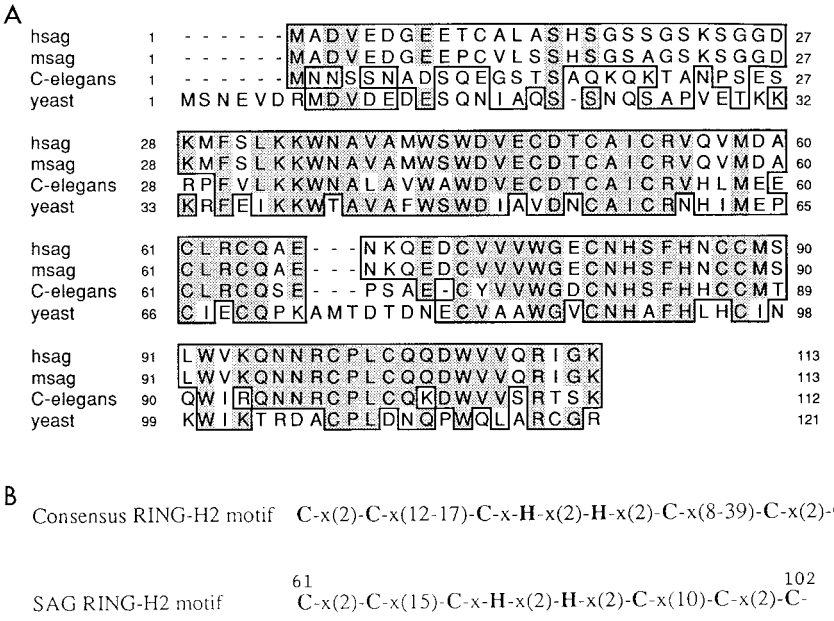

FIG. 1. SAG is evolutionarily conserved among different species. Primary amino acid sequences of human and mouse SAG were deduced from cDNAs cloned through DD and library screening. (A) Comparative alignments of SAG coding sequences from human, mouse, *C. elegans*, and yeast. Identity is shaded, and similarity is boxed. (B) Consensus sequence for the RING-H_2 motif and comparison of the zinc RING finger domain of SAG with the RING-H_2 motif. The $C_3H_2C_3$ residues are in boldface.

and freedom of mutations. To establish stable SAG-expressing lines, the pcDNA3-SAG or pcDNA3-Flag-SAG construct, respectively, was transfected by Lipofectamine (Bethesda Research Laboratories), along with the vector control, into DLD-1 human colon carcinoma cells or SY5Y human neuroblastoma cells that express a low level of endogenous SAG. After G418 (600 μg/ml) selection, stable clones were ring isolated and SAG expression was monitored by Northern analysis; selected clones were then examined for protein expression by immunoprecipitation or Western analysis. For 293 cells, transient transfection was performed by the calcium phosphate method as described previously (58).

DNA fragmentation assay. Subconfluent cells (80 to 90%) were treated with OP (150 μM) or $ZnSO_4$ (125 μM) for 24 h. Both detached and attached cells were harvested by scraping with a rubber policeman. Cells were collected by centrifugation and lysed in lysis buffer (5 mM Tris-HCl [pH 8], 20 mM EDTA, 0.5% Triton X-100) on ice for 45 min. Fragmented DNA in the supernatant after centrifugation at 14,000 rpm (45 min at 4°C) was extracted twice with phenol-chloroform and once with chloroform and then precipitated with ethanol and salt. The DNA pellet was washed once with 70% ethanol and resuspended in Tris-EDTA buffer with 100 μg of RNase per ml at 37°C for 2 h. The fragmented DNA was separated in 1.8% agarose gel electrophoresis, stained with ethidium bromide, and visualized under UV light (58).

TUNEL assay. The terminal deoxynucleotidyltransferase-mediated dUTP-biotin nick end labeling (TUNEL) assay was performed as instructed by the manufacturer (Boehringer Mannheim). Briefly, 5×10^4 cells were plated onto eight-well glass slides. After being treated with 1.25 mM copper ($CuSO_4$) or 200 μM zinc ($ZnSO_4$) for 16 h, cells were fixed with 0.5% glutaraldehyde for 10 min and then washed with PBS twice. The fixed cells were incubated in a permeabilization solution (0.1% Triton X-100, 0.1% sodium citrate) for 2 min on ice. The TUNEL reaction mixture (50 μl) was added to samples, which were incubated for 1 h at 37°C and then washed with PBS three times. Samples were embedded with antifade prior to analysis under a fluorescence microscope.

Nucleotide sequence accession numbers. The *SAG* sequences have been deposited in GenBank with accession no. AF092877 (mouse) and AF092878 (human). The cDNA clones have also been deposited in the American Type Culture Collection with assigned numbers 98402 (mouse) and 98405 (human).

RESULTS

Cloning of a novel protein that is evolutionarily conserved and contains a zinc RING finger domain. The DD technique was used in an attempt to isolate genes responsible for or associated with OP-induced apoptosis in two murine tumor lines (58). Two OP-inducible cDNA fragments were isolated. One encodes GSS, while the other is novel (57). The novel cDNA fragment was used as a probe to screen a mouse lung cDNA library. The resulting cDNA clone identified by this method contains a 1,140-bp insert encoding an open reading frame of 113 amino acids, including 12 cysteine residues (Fig. 1). The open reading frame was preceded by a 17-bp upstream sequence. An initiation codon was located in a context that conformed precisely 100% to the Kozak consensus sequence (34). The 3′-end untranslated region consists of 792 bp of sequence with two polyadenylation signals (AATAAA). Taken together, these features indicates that we have cloned a nearly full length cDNA. Since this clone was inducible in association with the OP-induced apoptosis pathway, we have named it *SAG*, for "sensitive to apoptosis gene."

To clone human *SAG* (*hSAG*), the mouse *SAG* (*mSAG*) cDNA was used as a probe to screen a HeLa cDNA library, and a 754-bp human clone was isolated. This clone encodes an open reading frame of 113 amino acids and contains a polyadenylation signal at the 3′-end untranslated region. Sequence identity between the mouse and human genes at the DNA level is 82% overall and 94% in the coding region. At the protein level, they show 96.5% identity. A database search revealed that these are novel genes but exhibit in the coding region 55% identity to yeast (accession no. Z74876) and 70% identity to *C. elegans* (accession no. U80449) hypothetical genes (Fig. 1A).

A motif search of the *SAG* open reading frame reveals a putative $C_3H_2C_3$ (RING-H_2) zinc RING finger domain at the C terminus of the molecule (Fig. 1B). The zinc RING finger protein belongs to a newly identified protein family (9), and RING-H_2-containing proteins have been identified in many species (for a list, see reference 27). The RING-H_2 domain identified in the products of the cloned *SAG* genes is completely conserved among the *C. elegans*, mouse, and human homologs. In yeast, only the last cysteine residue in $C_3H_2C_3$ motif is not conserved (Fig. 1B), which strongly suggests a functional role for this motif.

SAG is inducible by OP in mouse tumor cells. To confirm that *SAG* is subject to OP induction, we performed Northern

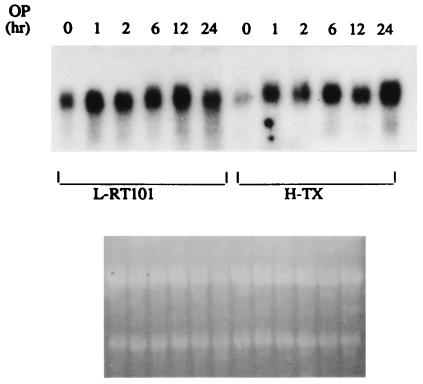

FIG. 2. SAG is inducible by OP. Subconfluent mouse L-RT101 and H-Tx cells were treated with OP (150 μM) for various periods of time up to 24 h and subjected to total RNA isolation and Northern analysis (with 15 μg of total RNA) using mouse SAG cDNA as a probe. Ethidium bromide staining of 28S and 18S rRNAs as loading controls is shown at the bottom.

analysis with RNAs isolated from two mouse tumor lines, L-RT101 (tumor promoter-transformed JB6 epidermal cells)(62) and H-Tx (spontaneously transformed mouse liver cells) (59a). As shown in Fig. 2, *mSAG* cDNA detects an OP-inducible transcript of 1.2 kb in size. Induction occurs 1 h after drug treatment and persists for up to 24 h in both cell lines, indicating that *SAG* is an early-response gene.

Tissue distribution and cellular and chromosomal localization of SAG. *hSAG* expression in several human tissues was examined. As shown in Fig. 3, *hSAG* was ubiquitously expressed in all tissues examined, although relatively low levels were detected in brain, placenta, lung, and kidney. Very high mRNA levels were detected in the heart, skeletal muscle, and testis (lanes 1, 6, and 12).

The cellular localization of hSAG was examined by immunofluorescent staining using a Myc-tagged antibody. As shown in Fig. 4A, hSAG is expressed in both the cytoplasm and nuclei of cells. As controls, the vector does not show any staining (Fig. 4B) and β-galactosidase is expressed mainly in the cytoplasm (Fig. 4C). The cytoplasm/nuclear localization of hSAG was also confirmed in a stable *hSAG* transfectant by using rabbit

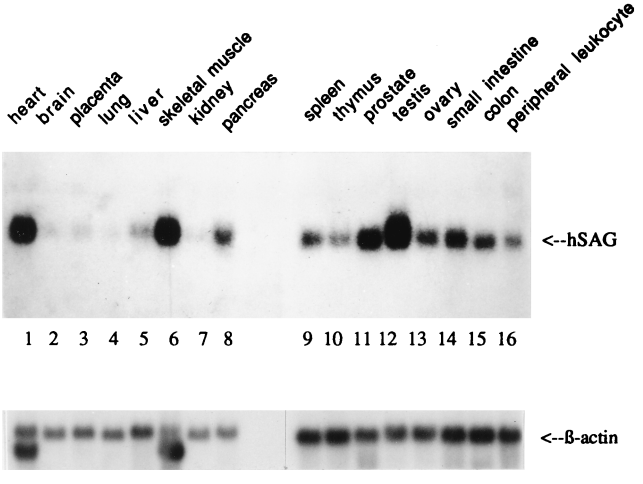

FIG. 3. SAG expression in multiple human tissues. *hSAG* cDNA was used as a probe for Northern analysis of poly(A)$^+$ RNA isolated from different human tissues (Clontech). For an internal loading control, the housekeeping β-actin gene was used (bottom).

anti-hSAG antibody (data not shown). Chromosomal localization of the *hSAG* gene was determined by SeeDNA Inc. (Toronto, Ontario, Canada), using the FISH mapping technique with *hSAG* cDNA as a probe. It is mapped to chromosome 3q22-24 (Fig. 4, bottom).

Biochemical characterization of hSAG. (i) SAG binds to metal ions. We first examined the biochemical activity of SAG. hSAG protein was expressed in bacteria and purified to near homogeneity (submitted for publication). Since SAG is a cysteine-rich protein containing a zinc RING finger domain, it has the potential to bind with metal ions. We used ESI-MS (17) to measure the potential zinc ion binding of SAG by comparing the molecular mass of SAG under denaturing and nondenaturing solution conditions (37, 72). Prior to ESI-MS analysis, urea-denatured pure SAG protein was dialyzed against 50 μM $ZnSO_4$ for 3 days with three changes of dialysis buffer. Higher concentrations of zinc solution were found to induce precipitation of the protein (data not shown). Under a denaturing acidic solution (pH 2.5 and high organic concentration) where the protein is not expected to retain metal binding characteristics even in the presence of zinc, the molecular mass of SAG was determined to be 12,550 Da, in close agreement with the expected mass for the apoprotein (12,552 Da) (Fig. 5A). ESI-MS analysis of the SAG protein in a nondenaturing aqueous solution (pH 7) resulted in higher masses of 12,733 and 12,800 Da (Fig. 5B), consistent for the holoprotein binding three and four zinc metal ions, respectively.

Copper ion binding to SAG was also investigated. As little as 1 μM $CuSO_4$ in the dialysis solution causes SAG precipitation with a blue (copper) color, suggesting copper binding (data not shown). Using ESI-MS, we then measured the potential copper binding of SAG in a nondenaturing solution as described above. Addition of copper acetate to a final concentration of 10 μM results in a further increase in mass to approximately 12,929 Da (data not shown). However, a precise mass could not be obtained, as a wide distribution of copper adducts appears to bind to SAG protein. Adding copper to higher concentrations resulted in precipitation of the protein.

(ii) SAG prevents LDL oxidation induced by copper ion or a free radical generator. Since SAG binds to metal ions, we reasoned that SAG may prevent metal ion-induced oxidation of macromolecules. Copper-induced oxidation of low-density lipoprotein (LDL) was used as a testing model. As shown in Fig. 6, copper-induced LDL oxidation, as measured by the formation of TBARS, is slightly enhanced by SAG at low concentrations. At higher SAG concentrations, however, a dose-dependent inhibition (up to 90%) of LDL oxidation is observed (Fig. 6A). Inhibition is heat resistant since heat-treated (60°C for 15 min) SAG retains the activity (Fig. 6B), suggesting that enzymatic activity is not involved. Inhibitory activity is, however, completely or partially abolished by pretreatment of SAG with the alkylating reagent *N*-ethylmaleimide or *p*-hydroxymercuric benzoate, respectively (Fig. 6B). The results indicate that free SH groups in the SAG molecule are the major contributors to this activity. Furthermore, MT, a small metal ion binding protein consisting of 20 cysteine residues out of 61 amino acids (44), shows an inhibitory curve similar to that for SAG (Fig. 6C). Glutathione, an additional cysteine-containing peptide, showed 25% inhibition at a concentration of 100 μM (data not shown). Inhibition of copper-induced LDL oxidation is, however, not observed in other known antioxidant enzymes such as superoxide dismutase or catalase or other proteins such as bovine serum albumin or cytochrome *c* (submitted for publication). These results clearly showed that by binding and chelating copper ion through its free SH groups, SAG prevents copper-initiated free radical

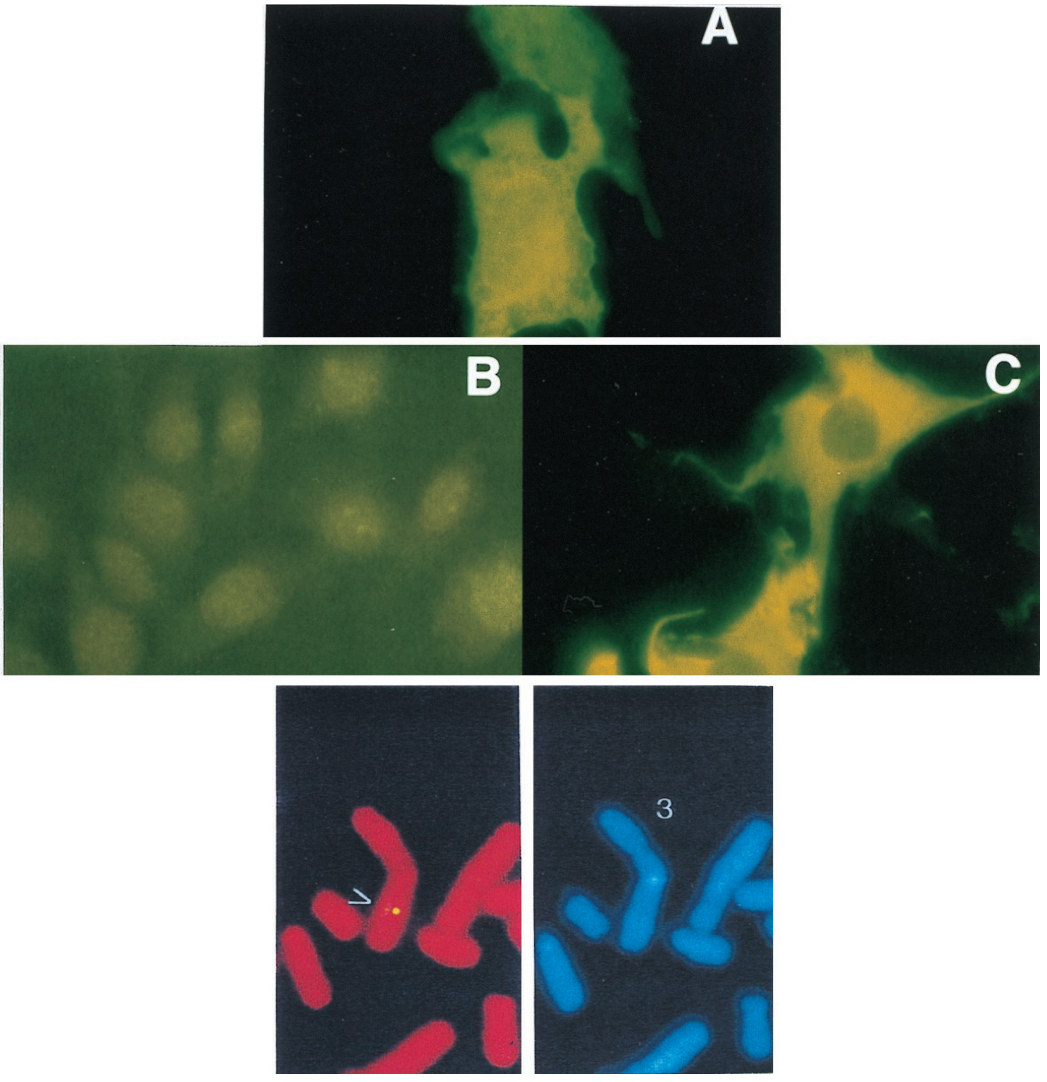

FIG. 4. Cellular and chromosomal localization of human SAG. (A to C) Cellular localization. NIH 3T3 cells were plated onto coverslips, transiently transfected with plasmid encoding SAG-Myc tag, and immunofluoresced by antibody against Myc tag as detailed in Materials and Methods. Shown are the SAG-expressing cells (A), vector control cells (B), and LacZ-expressing cells (C). FISH mapping (bottom) was done as detailed in Materials and Methods. Shown are the FISH signals on the chromosome (left) and the same mitotic figure stained with DAPI to identify chromosome 3 (right).

reactions leading to lipid peroxidation. Superoxide or hydrogen peroxide appears not to be involved in the process. To test whether protection of SAG against LDL oxidation is mediated solely through copper binding, we initiated LDL oxidation by AAPH, a free radical generator (21). In this metal ion-free system, SAG also inhibits LDL oxidation (up to 85%) at a concentration of 59 μM (750 μg/ml) (Fig. 6D). Thus, by metal binding and free radical scavenging, SAG acts as a protector against lipid peroxidation.

SAG protects cells from apoptosis induced by redox-sensitive reagents. Apoptosis has been widely implicated in human diseases such as cancers and neurodegenerative disorders (66). Since (i) *SAG* is inducible concurrent with the OP-induced apoptosis pathway, (ii) bacterially expressed SAG binds to metal ions, zinc, and copper, which also mediate apoptosis (19, 67), and (iii) bacterially expressed hSAG prevents copper or ROS-induced lipid peroxidation, we examined the potential role of SAG in redox-induced apoptosis. Several stable *hSAG* transfectants were generated in DLD-1 human colon carcinoma cells. Two transfectants (D12-1 and D12-8) showed high expression of SAG mRNA and protein compared to the neo controls (D1-3 and D1-6) (Fig. 7A). Sensitivity to apoptosis induced by OP as well as metal ions (zinc and copper) was examined by morphological appearance and DNA fragmentation. Treatment of cells with 150 μM OP or 125 μM $ZnSO_4$ for 24 h induced marked cell shrinkage and detachment in the neo control cells. These morphological signs of apoptosis were significantly reduced in SAG-expressing cells (data not shown). In the same treated cells, a DNA fragmentation ladder is clearly seen in two neo control lines (Fig. 7B [lanes 1 and 3] and C [lanes 1 and 2]) but significantly reduced in two SAG-overexpressing transfectants (Fig. 7B [lanes 2 and 4] and C [lanes 3 and 4]). In the case of copper sensitivity (up to 750 μM), expression of SAG does not offer significant protection when judged by morphological signs of apoptosis (not shown). Higher doses induce apoptosis in both lines (data not shown). These results indicated that when overexpressed, SAG pro-

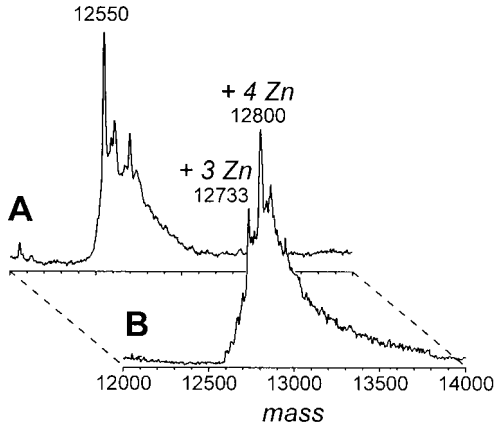

FIG. 5. SAG is a zinc binding protein. Shown are electrospray mass spectra of SAG protein in denaturing solvent (80:15:5 [vol/vol/vol] acetonitrile-water-acetic acid [pH 2.5]) (A) and nondenaturing solution (10 mM ammonium bicarbonate, 1 mM DTT [pH 7]) (B). The expected molecular mass of the apoprotein is 12,552 Da, with the first methionine deleted during expression and purification in bacteria. Assay conditions are detailed in Materials and Methods.

tected DLD-1 colon carcinoma cells from apoptosis induced by OP and zinc.

To examine a potential role of SAG in the protection against neuronal apoptosis, we transfected *hSAG* into SY5Y human neuroblastoma cells and selected stable lines that expressed exogenous SAG, as determined by Western blotting (Fig. 8A). One *hSAG* transfectant (SYW-20) and a vector control (SYV-3) were evaluated for sensitivity to the metal ions zinc and copper. As shown in Fig. 8B, SAG expression causes no morphological change in untreated cells (panels a and b). Treatment with 1.25 mM $CuSO_4$ (panels c and d) or 200 μM $ZnSO_4$ (panels e and f) for 16 h induces cell shrinkage and detachment in the neo control cells (panels c and e) but to a lesser extent in SAG-expressing cells (panels d and f). The morphological difference is more obvious with zinc treatment. To determine the nature of cell death, the TUNEL assay, a fluorescein labeling assay specific for free 3′-OH termini generated during cleavage of genomic DNA during apoptosis, was performed. As shown in Fig. 8C, substantially more fluorescein staining is seen in the vector control cells than that in hSAG-expressing cells after 16 h of treatment with either 1.25 mM $CuSO_4$ (compare panels c and d) or 200 μM $ZnSO_4$ (compare panels e and f). Results of the TUNEL assay agree well with

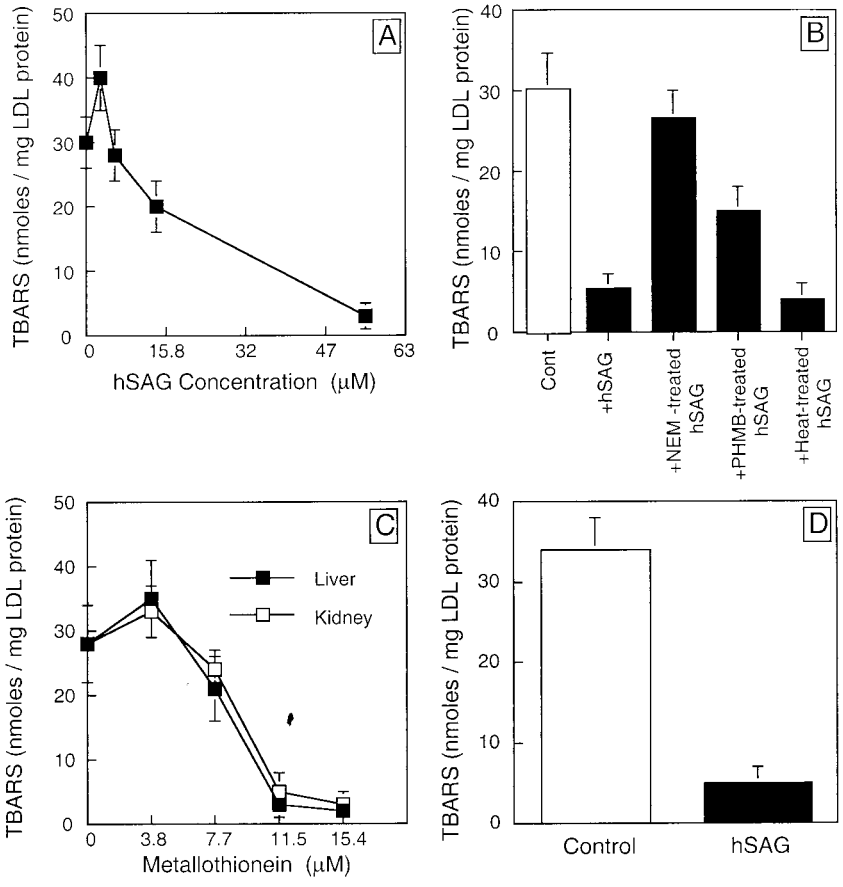

FIG. 6. SAG inhibits LDL oxidation induced by copper or AAPH. (A) Dose-dependent inhibition of copper-induced LDL oxidation by SAG. Different amounts of SAG protein were incubated with LDL in the presence of $CuSO_4$ (10 μM) for 10 min. Oxidation of LDL was measured by the formation of TBARS as detailed in Materials and Methods. (B) Abrogation of SAG protection by pretreatment with alkylating reagents but not by heat. SAG (750 μg/ml, 59 μM) was preincubated for 10 min with alkylating reagents *N*-ethylmaleimide (NEM; 50 mM) and *p*-hydroxymercuric benzoate (PHMB; 1 μmol/mg of SAG protein) or preheated (60°C for 15 min) before being subjected to LDL oxidation assay. Cont, control. (C) Dose-dependent inhibition of copper-induced LDL oxidation by MT. Different amounts of MT (from rabbit liver or horse kidney) were incubated with LDL in the presence of $CuSO_4$ (10 μM) for 10 min. Oxidation of LDL was measured by the formation of TBARS. (D) Inhibition of LDL oxidation induced by AAPH. SAG (750 μg/ml, 59 μM) was incubated with LDL in the presence of AAPH (5 mM) for 10 min. Formation of TBARS was measured as a index of LDL oxidation.

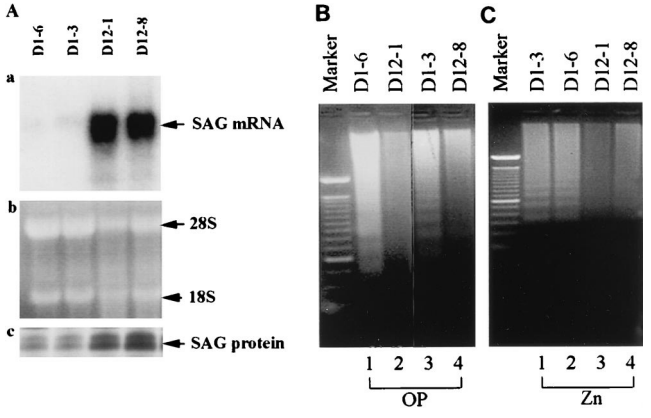

FIG. 7. Overexpression of hSAG protects DLD-1 colon carcinoma cells from apoptosis induced by OP and zinc. (A) Selection of SAG-expressing stable clones. DLD-1 cells were transfected with the neo control pcDNA3 or *hSAG* expression plasmid pcDNA-SAG. After G418 selection, resistant colonies were ring cloned and subjected to detection of exogenous SAG expression. (a) Expression of SAG mRNA. Total RNA was isolated and subjected to Northern analysis. Vector controls, D1-3 and D1-6; *hSAG* transfectants, D12-1 and D12-8. (b) 28S and 18S rRNAs for loading controls. (c) Expression of SAG protein in transfectants. The vector control lines and *hSAG* transfectants were subjected to immunoprecipitation. Shown is SAG protein expression in the neo controls (D1-3 and D1-6) and *hSAG* transfectants (D12-1 and D12-8). (B and C) hSAG overexpression protects cells from DNA fragmentation induced by OP or zinc. *hSAG* transfectants (D12-1 and D12-8), along with the vector control cells (D1-3 and D1-6), were seeded at 3.0×10^6 to 3.5×10^6 per 100-mm-diameter dish and exposed after 16 to 24 h to OP (150 μM; B) or zinc sulfate (125 μM; C) for 24 h. Both detached and attached cells in 2- by 100-mm dishes were harvested and subjected to DNA fragmentation assay. The 100-bp size marker is shown in the leftmost lane.

morphological observations, and both assays indicate a protective role of SAG in apoptosis induced by metal ions.

To examine SAG protection of an entire cell population against apoptosis, 293 human kidney cells were transiently transfected with an *hSAG* expression construct. Under our experimental conditions, 50 to 70% transfection efficiency can be reached with 293 cells (not shown). Twenty-four hours posttransfection, one set of transfectants was examined by Western blot analysis to confirm SAG expression (not shown), whereas the other set was exposed to $CuSO_4$ or $ZnSO_4$. SAG expression in these 293 cells protects against copper- but not zinc-induced morphological signs of apoptosis (data not shown). These results obtained from three independent human cell lines demonstrate that SAG acts as an antioxidant molecule to protect cells against apoptosis induced by redox agents. Protection against metal-induced apoptosis appears to be cell line dependent.

To examine whether SAG functions in antioxidant pathways mainly to inhibit apoptosis, SAG stable transfectants (DLD-1 and SY5Y) along with the vector controls were exposed to other common apoptosis inducers. Appearance of apoptosis was examined by morphological observation and DNA fragmentation assay. SAG protects cells only partially against apoptosis induced by etoposide (a DNA-damaging reagent) or UV but not at all against staurosporine-induced apoptosis (data not shown). Thus, SAG appears to play a role mainly in inhibiting apoptosis induced by redox agents.

Metal ions induce cytochrome *c* release and caspase activation that can be inhibited or delayed by SAG expression. Although metal ions have been shown to induce apoptosis through ROS generation, the mechanism of action underlying their effect is not clear. Since cytochrome *c* release from mitochondria and subsequent caspase activation are the key events in apoptosis (30, 35, 36, 43, 74), levels of cytochrome *c* released into the cytoplasm and potential activation of caspase were examined following treatment with metal ions. As shown in Fig. 9A (top), there is a low basal level of cytoplasmic cytochrome *c* in DLD-1 cells. Treatment of cells with 140 μM $ZnSO_4$ induces the release of cytochrome *c* into the cytoplasm. Densitometric analysis shows a 2.7- or 2.26-fold increase of cytoplasmic cytochrome *c* in the vector control D1-6 cells at 16 or 24 h posttreatment, respectively. In SAG-expressing D12-1 cells, an increase of cytoplasmic cytochrome *c* does not occur until 24 h and reaches a lower level (0.87- or 1.5-fold increase over the control at 16 or 24 h, respectively). Likewise, activation of caspase 7, inferred from the disappearance of the proenzyme form, is seen in a time-dependent manner after zinc treatment (bottom panel). More extensive activation (disappearance of the band) is observed in the vector-transfected cells (0.6- or 0.47-fold below that in untreated control at 16 or 24 h, respectively) than in SAG-expressing cells (1- or 0.68-fold lower than the control value at 16 h or 24 h, respectively). A similar result was obtained with caspase 3 activation (data not shown).

To further examine the potential protection by SAG against metal ion-induced cytochrome *c* release and caspase activation, we also measured cytochrome *c* release and caspase activation in 293 cells transiently transfected with the SAG-expressing plasmid following exposure to copper. As shown in Fig. 9B (top), a significant increase of cytochrome *c* release begins to occur 6 h after $CuSO_4$ (2.0 mM) treatment and lasts for up to 12 h (1-, 2.52-, 1.36-, 1.49-, or 0.97-fold increase at 0, 6, 8, 12, or 16 h posttreatment, respectively). Expression of SAG decreases as well as delays cytochrome *c* release (1-, 1.15-, 1.25-, 1.18-, or 1.02-fold increase at 0, 6, 8, 12, or 16 h, respectively). Significant activation of caspase 7 is seen in the vector control cells 12 and 16 h after copper treatment (1-, 0.91-, 0.95-, 0.75-, or 0.58-fold decrease at 0, 6, 8, 12, or 16 h, respectively). In contrast, no significant activation is seen in *hSAG* transfectants (1-, 1.09-, 1.2-, 1.08-, or 0.87-fold at 0, 6, 8, 12, or 16 h, respectively) (bottom panel). Similar results were seen with caspase 3 activation (data not shown). These results indicate that metal ion treatment induces cytochrome *c* release and caspase activation during apoptosis which can be largely inhibited or delayed by SAG overexpression.

DISCUSSION

SAG is a novel member of the zinc RING finger family of proteins. Using the DD technique, we identified an OP-inducible gene, *SAG*, that encodes a novel protein containing zinc RING finger domain. Zinc RING finger genes represent is a new and growing family of genes (20, 52) whose members contain C_3HC_4 or $C_3H_2C_3$ (a cysteine-to-histidine change) motif and are involved biochemically in DNA binding, RNA binding, and protein-protein interactions (8, 9, 16, 38). Biologically, the zinc RING finger proteins are involved in many processes, including oncogenesis, signal transduction, and development, among others (52). Some RING finger proteins, including the baculovirus protein p35 and mammalian homologs of baculovirus inhibitors of apoptosis, are known to inhibit apoptosis (13, 63, 68). SAG, described here, consists of 113 amino acids with 12 cysteine residues. It is the smallest of the RING finger proteins, with 50% of the polypeptide consisting of a RING domain. The protective activity against redox-induced apoptosis renders SAG the first antioxidant molecule among RING finger family members.

SAG is evolutionarily conserved and expressed highly in energy-consuming organs. SAG is evolutionarily conserved,

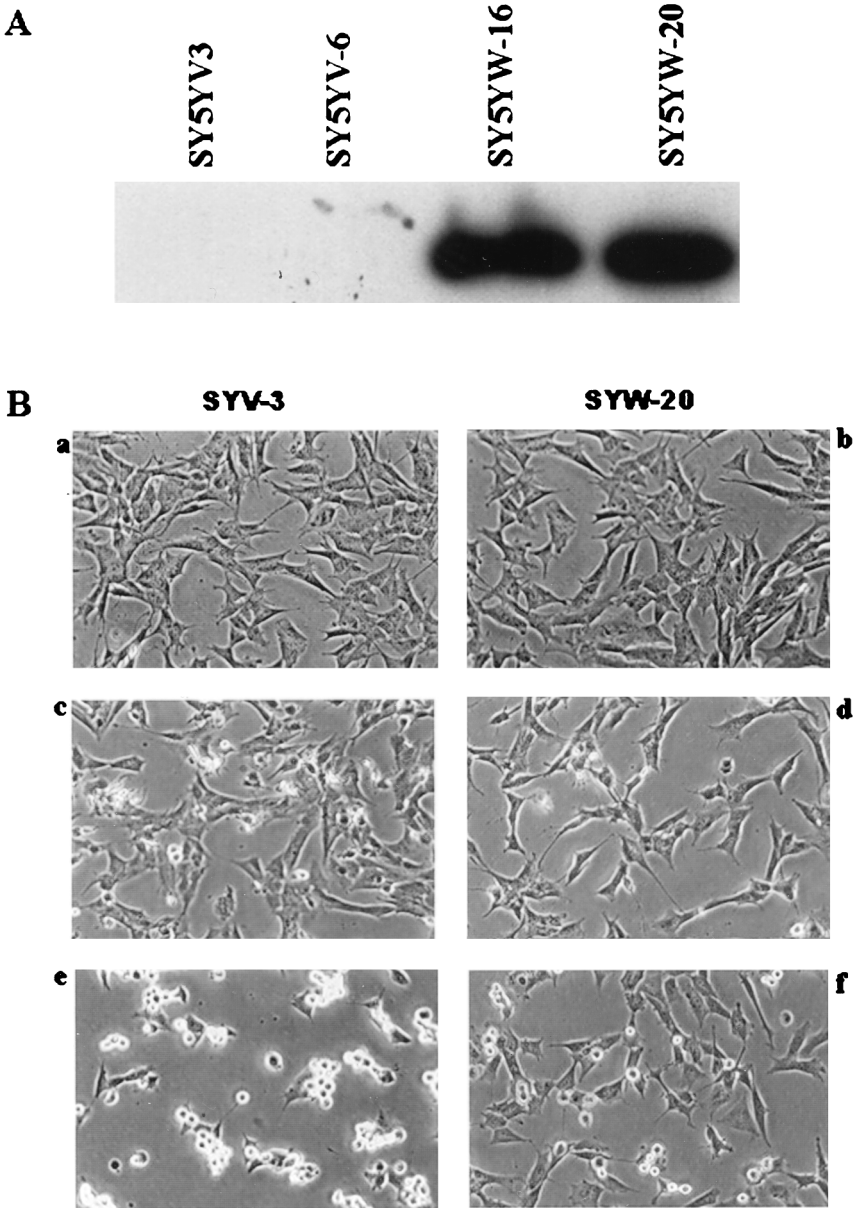

FIG. 8. Overexpression of hSAG protects SY5Y neuroblastoma cells from apoptosis induced by copper and zinc. (A) Selection of SAG-expressing stable clones. SY5Y cells were transfected with the neo control pcDNA3 or *hSAG* expression plasmid pcDNA-Flag-SAG. After G418 selection, resistant cell lines were ring cloned and subjected to Western blot analysis for exogenous SAG expression with anti-Flag antibody. (B) Protection of metal-induced apoptosis as shown by morphological appearance. SAG-expressing cells (SYW20 [b, d, and f]) and neo control cells (SYV3 [a, c, and e]) were untreated (a and b) or exposed to $CuSO_4$ (1.25 mM [c and d]) or $ZnSO_4$ (200 μM [e and f]) for 16 h. Morphology was visualized at a magnification of ×200. (C) Protection of metal-induced apoptosis as shown by TUNEL assay. Cells were exposed to metal ions for 16 h as described above (without treatment [a and b]; with 1.25 mM $CuSO_4$ [c and d]; with 200 μM $ZnSO_4$ [e and f]), then subjected to TUNEL assay as detailed in Materials and Methods, and analyzed under a fluorescence microscope with a blue filter. Magnification, ×200.

with 55 or 70% identity, respectively, between human and yeast or human and *C. elegans* sequences. High sequence homology often suggests a functional conservation, as seen in many other proteins, including the apoptosis-related proteins Bcl-2, Apaf-3/caspase 9, and Apaf-1 and their *C. elegans* homologs, ced-9, ced-3, and ced-4, respectively (35, 69, 75). Indeed, *hSAG* and *ySAG* (yeast homolog of *hSAG*) have similar functions: yeast lethality induced by disruption of *ySAG* can be fully complemented by *hSAG* (unpublished data). Thus, *hSAG* could be a growth-essential gene by functioning as an antioxidant molecule to protect cells against ROS-induced death or by promoting cell growth through other mechanisms (unpublished data).

Consistent with its antioxidant activity, SAG is expressed at high levels in human heart, skeletal muscle, and testis. These three organs consist of either muscle cells for contraction or sperm cells for mobility. The cellular movement in these organs requires much higher amounts of oxygen, resulting in high collateral levels of ROS. It is conceivable, therefore, that these organs express a high constitutive level of SAG as a defense against ROS-induced damage. Accordingly, the striated myofibers in skeletal muscle and heart are long-lived cells, while several inherited muscle diseases, including muscular dystrophy and spinal muscle atrophy, are characterized by degeneration of muscle fibers through apoptosis and necrosis (18, 65).

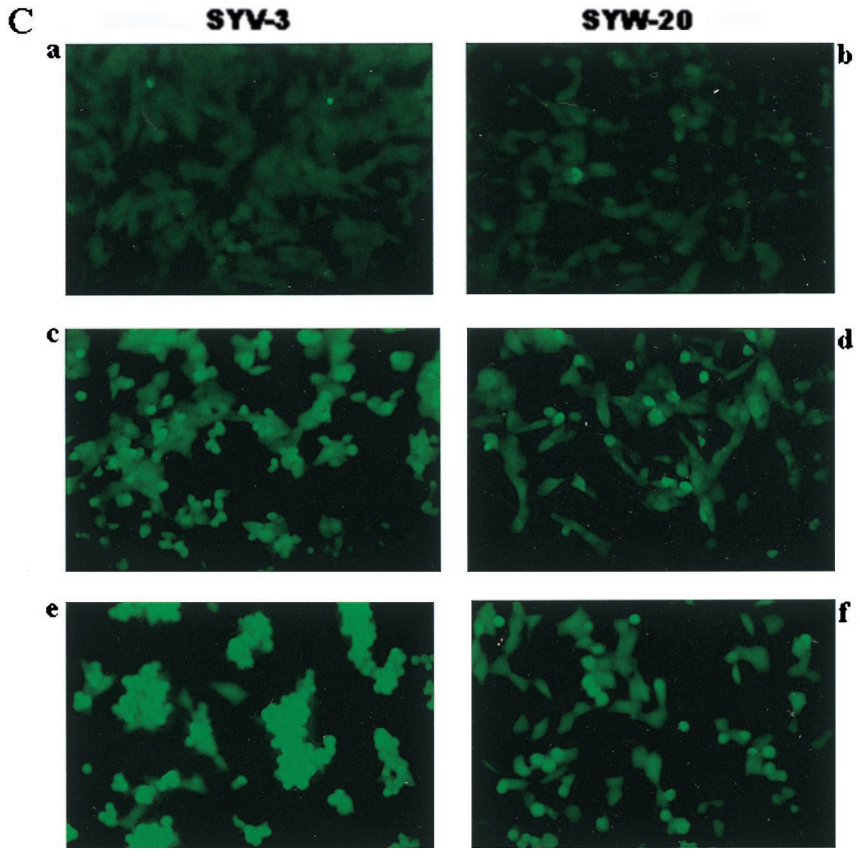

FIG. 8—*Continued.*

It will be of great interest to examine SAG expression in these diseased cells.

***SAG* is an antioxidant molecule that inhibits apoptosis in multiple human tumor lines.** In an attempt to isolate genes that mediate OP-induced apoptosis (58), we used the DD technique and isolated two OP-inducible genes. The first gene encodes GSS, the enzyme involved in the last step of glutathione synthesis (57), and the second is *SAG*. Both seem to be involved in antioxidant pathways that counteract rather than potentiate OP-induced apoptosis (reference 57 and this report). Induction of *GSS* and *SAG*, therefore, appears to be a cellular defense response against OP-induced redox disturbance. When this disturbance is dominant and overcomes the protective response, cells eventually undergo apoptosis. In addition to being inducible by the redox agent OP in mouse cell lines, *SAG* was also induced in mouse brain after ischemia damage (unpublished observation). Thus, *SAG* appears to be a stress-responsive gene in cells that acts as a protector against ROS-induced damage.

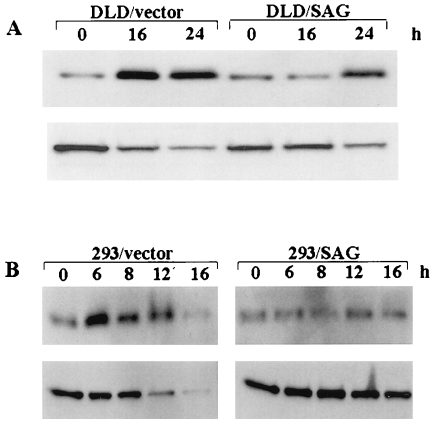

FIG. 9. Overexpression of SAG inhibits or delays metal ion-induced cytochrome *c* release and caspase activation. (A) SAG-expressing DLD cells (D12-1) and neo control cells (D1-6) were subjected to $ZnSO_4$ (140 μM) treatment for the indicated periods of time. The cytoplasmic fraction was extracted and subjected to Western blot analysis with antibodies against cytochrome *c* (top) and caspase 7 (bottom). (B) Human 293 cells were transiently transfected with *hSAG* expression plasmid or the neo control. Twenty-four hours posttransfection, cells were treated with $CuSO_4$ (2 mM) for the indicated periods of time and subjected to Western blot analysis with antibodies against cytochrome *c* (top) and caspase 7 (bottom). Densitometric quantitation was performed in a densitometer. The band density from the untreated control was arbitrarily chosen as 1.

Metal chelators and metal ions have been shown to induce apoptosis through ROS generation. Under our experimental conditions, OP, Cu^{2+}, or Zn^{2+} alone induces apoptosis in DLD-1 colon carcinoma cells, SY5Y neuroblastoma cells, or 293 cells, as evidenced by morphological appearance, TUNEL assay, and DNA fragmentation. SAG, when overexpressed in these cells, plays a protective role, although the degree of protection against each reagent varies among the tested cell lines. How does SAG function as an inhibitor of redox-induced apoptosis? In vitro biochemical analysis could provide a clue. Bacterially expressed and purified hSAG has metal ion binding activity. This is likely mediated by cysteine residues (a total of 12) as well as histidine residues (a total of three) in SAG molecule. The fact that SAG binds to three or four zinc ions but the zinc RING finger structure would predict binding of only two zinc ions may imply that in vitro-purified SAG does

not adapt a RING finger conformation or that other cysteine or histidine residues not involved in the RING structure also bind to zinc. As a result of copper binding, SAG prevents copper-induced LDL oxidation which is the result of a radical chain reaction initiated by Cu^{2+} reduction. The same activity but with a higher specificity was detected by using MT, a cysteine-rich small protein which was found to bind with seven metal ions per molecule (45). A similar dose-dependent inhibition curve between SAG and MT suggests that the reaction follows similar kinetics. It is conceivable that a lower concentration of MT than of SAG is needed to achieve the same degree of inhibition due to MT's higher content of cysteine residues and higher capacity for metal binding per molecule. It is not clear, however, why at a low concentration both SAG and MT stimulate lipid peroxidation under this experimental condition. In addition to inhibiting copper-induced LDL oxidation, SAG also inhibits lipid peroxidation induced by AAPH, a free radical generator. Thus, SAG binds to copper to prevent initiation of radical reactions as well as scavenges the radicals to terminate the reaction. Furthermore, subcellular localization of SAG in both the cytoplasm and the nucleus makes it readily accessible to metal ions and ROS generated during oxidative stress.

We observed that the sensitivity to metal ions and protection by SAG were cell density as well as cell line dependent. In general, cells at a higher density can tolerate a higher concentration of metal ions, particularly zinc due to cell-cell communication. The cell line dependence could result from differences in cellular redox buffering capacity, including levels of other antioxidant molecules as well as the balance of prooxidants and antioxidants in these cells. It is noteworthy that there is a very narrow range of concentration in metal ion-induced apoptosis. A slight increase of metal ion concentration above the threshold would lead to a marked appearance of apoptosis. As expected, SAG could protect cells only up to a certain level, above which the protective effect was abolished. It is conceivable that zinc and copper are trace elements in cells and OP is not present. Exogenous challenge with excess metal ions or a redox agent could induce a series of cellular responses. If the concentration was beyond tolerable levels, apoptosis would occur rapidly, as seen in OP-induced apoptosis (58), even though both GSS and SAG were induced (57).

Since apoptosis is mediated in many cases by cytochrome *c* release followed by caspase activation (30, 35, 36, 43, 74), we examined this signaling pathway in a metal ion-induced apoptosis model. We showed, for the first time, that either zinc or copper would induce cytochrome *c* release and caspase activation. How do metal ions induce cytochrome *c* release? The simplest explanation is that metal ions trigger ROS generation followed by mitochondrial membrane damage that leads to cytochrome *c* release. Additional studies on mitochondrial membrane integrity and permeability following exposure to metal ions needs to be conducted to understand the process. Bcl-2, a well-known apoptosis inhibitor, blocks cytochrome *c* release from mitochondria in cells undergoing apoptosis (30, 74). Bcl-2 has also been shown to inhibit apoptosis in an antioxidant pathway (25). Difference in subcellular localization between SAG (cytoplasm and nucleus) and Bcl-2 (mitochondria and endoplasmic reticulum) may determine their antioxidant functions at different organelles. In addition to antioxidant activity, Bcl-2 also possesses pore-forming properties that prevent cytochrome *c* release (54). Protection by SAG against cytochrome *c* release and caspase activation is most likely to operate through its metal ion binding and radical scavenging activities.

In summary, we have cloned and characterized a novel, evolutionarily conserved antioxidant protein, SAG, that in vitro binds to metal ions and inhibits lipid peroxidation and in vivo protects cells from redox-induced apoptosis. Based on its tissue distribution and biological functions, SAG could have potential therapeutic applications in diseases such as cancers (66), neurodegenerative disorders (66), stroke (32), and muscular dystrophy (18, 65).

ACKNOWLEDGMENTS

We thank Steve Hunt (Parke-Davis) for helpful discussion and Paul Miller (Pfizer Central Research) for critical reading of the manuscript.

REFERENCES

1. **Abello, P. A., S. A. Fidler, G. B. Bulkley, and T. G. Buchman.** 1994. Antioxidants modulate induction of programmed endothelial cell death (apoptosis) by endotoxin. Arch. Surg. **129:**134–141.
2. **Adebodun, F., and J. F. Post.** 1995. Role of intracellular free Ca(II) and Zn(II) in dexamethasone-induced apoptosis and dexamethasone resistance in human leukemic CEM cell lines. J. Cell. Physiol. **163:**80–86.
3. **Allen, R. G., and A. K. Balin.** 1989. Oxidative influence in development and differentiation: an overview of a free radical theory of development. Free Radical Biol. Med. **6:**631–661.
4. **Auld, D. S.** 1988. Use of chelating agents to inhibit enzymes. Methods Enzymol. **158:**110–114.
5. **Baker, A., C. M. Payne, M. M. Briehl, and G. Powis.** 1997. Thioredoxin, a gene found overexpressed in human cancer, inhibits apoptosis in vitro and in vivo. Cancer Res. **57:**5162–5167.
6. **Beg, A. A., and D. Baltimore.** 1996. An essential role for NF-κB in preventing TNF-α induced cell death. Science **274:**782–784.
7. **Bessho, R., K. Matsubara, M. Kubota, K. Kuwakado, H. Hirota, Y. Wakazono, Y. W. Lin, A. Okada, M. Kawai, and R. Nishikomori.** 1994. Pyrrolidine dithiocarbamate, a potent inhibitor of nuclear factor κB (NF-κB) activation, prevents apoptosis in human promyelocytic leukemia HL-60 cells and thymocytes. Biochem. Pharmacol. **48:**1883–1889.
8. **Boddy, M. N., P. S. Freemont, and K. L. B. Borden.** 1994. The p53-associated protein MDM2 contains a newly characterized zinc-binding domain called the RING finger. Trends Biochem. Sci. **19:**198–199.
9. **Borden, K. L. B., and P. S. Freemont.** 1996. The ring finger domain: a recent example of a sequence-structure family. Curr. Opin. Struct. Biol. **6:**395–401.
10. **Buege, J. A., and S. D. Aust.** 1976. Microsomal lipid peroxidation. Methods Enzymol. **52:**302–310.
11. **Burkitt, M. J., L. Milne, P. Nicotera, and S. Orrenius.** 1996. 1,10-Phenathroline stimulates internucleosomal DNA fragmentation in isolated rat-liver nuclei by promoting the redox activity of endogenous copper ions. Biochem. J. **313:**163–169.
12. **Chio, D. W., M. Yokoyama, and J. Koh.** 1988. Zinc neurotoxicity in cortical cell culture. Neuroscience **24:**67–79.
13. **Clem, R. J., and L. K. Miller.** 1994. Control of programmed cell death by the baculovirus genes *p35* and *iap*. Mol. Cell. Biol. **14:**5212–5222.
14. **deHaan, J. B., F. Cristiano, R. Ianello, C. Bladier, M. J. Kelner, and I. Kola.** 1996. Elevation in the ratio of Cu/Zn superoxide dismutase to glutathione peroxidase activity induces features of cellular senescence and this effect is mediated by hydrogen peroxide. Hum. Mol. Genet. **5:**283–292.
15. **Duan, H., A. M. Chinnaiyan, P. L. Hudson, J. P. Wing, W.-W. He, and V. M. Dixit.** 1996. ICE-LAP3, a novel mammalian homologue of the Caenorhabditis elegans cell death protein Ced-3 is activated during Fas- and tumor necrosis factor-induced apoptosis. J. Biol. Chem. **271:**1621–1625.
16. **Elenbass, B., M. Dobbelstein, J. Roth, T. Shenk, and A. J. Levine.** 1996. The MDM2 oncoprotein binds specifically to RNA through its RING finger domain. Mol. Med. **2:**439–451.
17. **Fenn, J. B., M. Mann, C. K. Meng, S. F. Wong, and C. M. Whitehouse.** 1989. Electrospray ionization for mass spectrometry of large biomolecules. Science **246:**64–71.
18. **Fidzianska, A., H. H. Goebel, and I. Warlo.** 1990. Acute infantile spinal muscular atrophy. Muscle apoptosis as a proposed pathogenetic mechanism. Brain **113:**433–445.
19. **Fraker, P. J., and W. G. Telford.** 1997. A reappraisal of the role of zinc in life and death decision of cells. Proc. Soc. Exp. Biol. Med. **215:**229–236.
20. **Freemont, P. S., I. M. Hanson, and J. Trowsdale.** 1991. A novel cystein-rich sequence motif. Cell **64:**483–484.
21. **Frei, B., R. Stocker, and B. N. Ames.** 1988. Antioxidant defenses and lipid peroxidation in human blood plasma. Proc. Natl. Acad. Sci. USA **85:**9748–9752.
22. **Heng, H. H. Q., J. Squire, and L. C. Tsui.** 1992. High resolution mapping of mammalian genes by in situ hybridization to free chromatin. Proc. Natl. Acad. Sci. USA **89:**9509–9513.
23. **Heng, H. H. Q., and L. C. Tsui.** 1993. Modes of DAPI banding and simultaneous in situ hybridization. Chromosoma **102:**325–332.
24. **Hiraku, Y., and S. Kawanishi.** 1996. Oxidative DNA damage and apoptosis

induced by benzene metabolites. Cancer Res. **56:**5172–7178.
25. **Hockenbery, D. M., Z. N. Oltwai, X. M. Yin, C. L. Milliman, and S. J. Korsmeyer.** 1993. Bcl-2 functions in an antioxidant pathway to prevent apoptosis. Cell **22:**241–251.
26. **Hughes, F. M., Jr., and J. A. Cidlowski.** 1994. Regulation of apoptosis in S49 cells. J. Steroid Biochem. Mol. Biol. **49:**303–310.
27. **Inouye, C., N. Dhillon, and J. Thorner.** 1997. Ste5 RING-H2 domain: role in Ste4-promoted oligomerization for yeast pheromone signaling. Science **278:** 103–106.
28. **Jacobson, M. D.** 1996. Reactive oxygene species and program cell death. Trends Biochem. Sci. **21:**83–86.
29. **Kayanoki, Y., J. Fujii, K. N. Islam, K. Suzuki, S. Kawata, Y. Matsuzawa, and N. Taniguchi.** 1996. The protective role of glutathione peroxidase in apoptosis induced by reactive oxygen species. J. Biochem. **119:**817–822.
30. **Kluck, R. M., E. Bossy-Wetzel, D. R. Green, and D. D. Newmeyer.** 1997. The release of cytochrome c from mitochondria: a primary site for Bcl-2 regulation of apoptosis. Science **275:**1132–1136.
31. **Koh, J.-Y., and D. W. Choi.** 1994. Zinc toxicity on cultured cortical neurons: involvement of N-methyl-D-aspartate receptors. Neuroscience **60:**1049–1057.
32. **Koh, J.-Y., S. Suh, B. Gwag, Y. He, C. Hsu, D. W. Choi.** 1996. The role of zinc in selective neuronal death after transient global cerebral ischemia. Science **272:**1013–1016.
33. **Kondo, Y., J. M. Rusnak, D. G. Hoyt, C. E. Settineri, B. R. Pitt, and J. S. Lazo.** 1997. Enhanced apoptosis in metallothionein null cells. Mol. Pharmacol. **52:**195–201.
34. **Kozak, M.** 1991. Structural features in eukaryotic mRNAs that modulate the initiation of translation. J. Biol. Chem. **266:**19867–19870.
35. **Li, P., D. Nijhawan, I. Budihardjo, S. M. Srinivasula, M. Ahmad, E. S. Alnemri, and X. Wang.** 1997. Cytochrome c and dATP-dependent formation of Apaf-1/caspase-9 complex initiates an apoptotic protease cascade. Cell **91:**479–489.
36. **Liu, X., C. N. Kim, J. Yang, R. Jemmerson, and X. Wang.** 1996. Induction of apoptotic program in cell-free extracts: requirement for dATP and cytochrome c. Cell **86:**147–157.
37. **Loo, J. A.** 1997. Studying noncovalent protein complexes by electrospray ionization mass spectrometry. Mass Spectrom. Rev. **16:**1–23.
38. **Lovering, R., I. M. Hanson, K. L. B. Bordern, S. Martin, N. J. O'Reilly, G. I. Evan, D. Rahman, D. J. C. Pappin, J. Trowsdale, and P. S. Freemont.** 1993. Identification and preliminary characterization of a protein motif related to the zinc finger. Proc. Natl. Acad. Sci. USA **90:**2112–2116.
39. **Manev, H., E. Kharlamov, T. Uz, R. P. Mason, and C. M. Cagnoli.** 1997. Characterization of zinc-induced neuronal death in primary cultures of rat cerebellar granule cells. Exp. Neurol. **146:**171–178.
40. **Manna, S. K., H. J. Zhang, T. Yan, L. W. Oberley, and B. B. Aggarwal.** 1998. Overexpression of manganese superoxide dismutase suppresses tumor necrosis factor-induced apoptosis and activation of nuclear transcription factor-kappaB and activated protein-1. J. Biol. Chem. **273:**13245–13254.
41. **Mariani, S. M., B. Matiba, C. Baumler, and P. H. Krammer.** 1995. Regulation of cell surface APO-1/Fas (CD95) ligand expression by metalloproteases. Eur. J. Immunol. **25:**2303–2307.
42. **Mayo, M. W., C.-Y. Wang, P. C. Cogswell, K. S. Rogers-Graham, S. W. Lowe, C. J. Der, and A. S. Baldwin, Jr.** 1997. Requirement of NF-κB activation to suppress p53-independent apoptosis induced by oncogenic Ras. Science **278:** 1812–1815.
43. **Mignotte, B., and J.-L. Vayssiere.** 1998. Mitochondria and apoptosis. Eur. J. Biochem. **252:**1–15.
44. **Nordberg, M.** 1986. Metallothionein deserves attention. Prog. Clin. Biol. Res. **214:**401–410.
45. **Otvos, J. D., and I. M. Armitage.** 1980. Structure of the metal clusters in rabbit liver metallothionein. Proc. Natl. Acad. Sci. USA **77:**7094–7098.
46. **Paramanantham, R., K. H. Sit, and B. H. Bay.** 1997. Adding Zn^{2+} induces DNA fragmentation and cell condensation in cultured human Chang liver cells. Biol. Trace Elem. Res. **58:**135–147.
47. **Perry, D. K., M. J. Smyth, H. R. Stennicke, G. S. Salvesen, P. Duriez, G. G. Poirier, and Y. A. Hannun.** 1997. Zinc is a potent inhibitor of the apoptotic protease, caspase-3: a novel target for zinc in the inhibition of apoptosis. J. Biol. Chem. **272:**18530–18533.
48. **Polyak, K., Y. Xia, J. L. Zweier, K. W. Kinzler, and B. Vogelstein.** 1997. A model for p53-induced apoptosis. Nature **389:**300–305.
49. **Provinciali, M., G. D. Stefano, and N. Fabris.** 1995. Dose-dependent opposite-effect of zinc on apoptosis in mouse thymocytes. Int. J. Immunopharmacol. **17:**735–744.
50. **Sannes-Lowery, K. A., P. Hu, D. P. Mack, H.-Y. Mei, and J. A. Loo.** 1997. HIV-1 tat peptide binding to TAR RNA by electrospray ionization mass spectrometry. Anal. Chem. **69:**5130–5135.
51. **Satoh, K., T. Kadofuku, and H. Sakagami.** 1997. Copper, but not iron, enhances apoptosis-inducing activity of antioxidants. Anticancer Res. **17:**2487–2490.
52. **Saurin, A. J., K. L. B. Border, M. N. Boddy, and P. S. Freemont.** 1996. Does this have a familiar RING? Trends Biochem. Sci. **21:**208–214.
53. **Sawada, T., S. Hashimoto, H. Furukawa, S. Tohma, T. Inoue, and K. Ito.** 1997. Generation of reactive oxygen species is required for bucillamine, a novel anti-rheumatic drug, to induce apoptosis in concert with copper. Immunopharmacology **35:**195–202.
54. **Schendel, S. L., Z. Xie, M. O. Montal, S. Matsuyama, M. Montal, and J. C. Reed.** 1997. Channel formation by antiapoptotic protein Bcl-2. Proc. Natl. Acad. Sci. USA **94:**5113–5118.
55. **Shibanuma, M., T. Kuroki, and K. Nose.** 1990. Stimulation by hydrogen peroxide of DNA synthesis, competence family gene expression and phosphorylation of a specific protein in quiescent Balb/3T3 cells. Oncogene **5:**1025–1032.
56. **Sun, Y.** 1990. Free radicals, antioxidant enzymes, and carcinogenesis. Free Radical Biol. Med. **8:**583–599.
57. **Sun, Y.** 1997. Induction of glutathione synthetase by 1,10-phenanthroline. FEBS Lett. **408:**16–20.
58. **Sun, Y., J. Bian, Y. Wang, and C. Jacobs.** 1997. Activation of p53 transcriptional activity by 1,10-phenanthroline, a metal chelator and redox sensitive compound. Oncogene **14:**385–393.
59. **Sun, Y., G. Hegamyer, and N. H. Colburn.** 1994. Molecular cloning of five messenger RNAs differentially expressed in preneoplastic or neoplastic JB6 mouse epidermal cells: one is homologous to human tissue inhibitor of metalloproteinases-3. Cancer Res. **54:**1139–1144.
59a. **Sun, Y., G. Hegamyer, K. Nakamurra, H. Kim, L. W. Oberley, and N. H. Colburn.** 1993. Alterations of the p53 tumor-suppressor gene in transformed mouse liver cells. Int. J. Cancer **55:**952–956.
60. **Sun, Y., K. Nakamura, G. A. Hegamyer, Z. G. Dong, and N. H. Colburn.** 1993. No point mutation of H-*ras* or p53 genes expressed in preneoplastic-to neoplastic progression as modeled in mouse JB6 cell variants. Mol. Carcinog. **8:**49–57.
61. **Sun, Y., and L. W. Oberley.** 1996. Redox regulation of transcriptional activators. Free Radical Biol. Med. **21:**335–348.
62. **Sun, Y., Y. Pommier, and N. H. Colburn.** 1992. Acquisition of a growth-inhibitory response to phorbol ester involves DNA damage. Cancer Res. **52:**1907–1915.
63. **Takahashi, R., Q. Deveraux, I. Tamm, K. Welsh, N. Assa-Munt, G. S. Salvesen, and J. C. Reed.** 1998. A single BIR domain of XIAP sufficient for inhibiting caspases. J. Biol. Chem. **273:**7787–7790.
64. **Tan, S., Y. Sagara, Y. Liu, P. Maher, and D. Schubert.** 1998. The regulation of reactive oxygen species production during programmed cell death. J. Cell Biol. **141:**1423–1432.
65. **Tews, D. S., H. H. Goebel, and H. M. Meinck.** 1997. DNA-fragmentation and apoptosis-related proteins of muscle cells in motor neuron disorders. J. Neuropathol. Exp. Neurol. **56:**150–156.
66. **Thompson, C. B.** 1995. Apoptosis in the pathogenesis and treatment of disease. Science **267:**1456–1462.
67. **Tsang, S. Y., S. C. Tam, I. Bremner, and M. J. Burkitt.** 1995. Copper-1,10-phenanthroline induces internucleosomal DNA fragmentation in HepG2 cells, resulting from direct oxidation by the hydroxyl radical. Biochem. J. **317:**13–16.
68. **Uren, A. G., M. Pakush, C. J. Hawkins, K. L. Puls, and D. L. Vaux.** 1996. Cloning and expression of apoptosis inhibitory protein homologs that function to inhibit apoptosis and/or bind tumor necrosis factor receptor-associated factors. Proc. Natl. Acad. Sci. USA **93:**4974–4978.
69. **Vaux, D. L., I. L. Weissman, and S. K. Kim.** 1992. Prevention of programmed cell death in Caenorhabditis elegans by human bcl-2. Science **258:**1955–1957.
70. **Wang, T.-S., C.-F. Kuo, K.-Y. Jan, and H. Huang.** 1996. Arsenite induces apoptosis in Chinese hamster ovary cells by generation of reactive oxygen species. J. Cell. Physiol. **169:**256–268.
71. **Wolfe, J. T., D. Ross, and G. M. Cohen.** 1994. A role for metals and free radicals in the induction of apoptosis in thymocytes. FEBS Lett. **352:**58–62.
72. **Witkowska, H. E., C. H. L. Shackleton, K. Dahlman-Wright, J. Y. Kim, and J.-A. Gustafsson.** 1995. Mass spectrometric analysis of a native zinc-finger structure: the glucocorticoid receptor DNA binding domain. J. Am. Chem. Soc. **117:**3319–3324.
73. **Wyllie, A. H.** 1980. Glucocorticoid-induced thymocyte apoptosis is associated with endogenous endonuclease activation. Nature **284:**555–556.
74. **Yang, J., X. Liu, K. Bhalla, C. N. Kim, A. M. Ibrado, J. Cai, T.-I. Peng, D. P. Jones, and X. Wang.** 1997. Prevention of apoptosis by bcl-2: release of cytochrome c from mitochondria blocked. Science **275:**1129–1132.
75. **Zou, H., W. J. Henzel, X. Liu, A. Lutschg, and X. Wang.** 1997. Apaf-1, a human protein homologous to C. elegans CED-4, participates in cytochrome c-dependent activation of caspase-3. Cell **90:**405–413.